

Magnetization behavior and magnetic viscosity in nanostructured $\text{PrCo}_{4.5}\text{C}_{0.5}$ ribbons

Bai Yang, Bao-Gen Shen,^{a)} Tong-Yun Zhao, and Ji-Rong Sun

State Key Laboratory of Magnetism, Institute of Physics and Beijing National Laboratory for Condensed Matter Physics, Chinese Academy of Sciences, Beijing 100190, People's Republic of China

(Received 25 December 2007; accepted 9 April 2008; published online 20 June 2008)

The magnetization processes in nanocomposite $\text{PrCo}_{4.5}\text{C}_{0.5}$ ribbons that are composed of two hard magnetic phases $\text{PrCo}_5\text{C}_\delta$ and $\text{Pr}_5\text{Co}_{19}\text{C}_\epsilon$ have been systematically investigated. The magnetic reversal of the samples is found to be mainly determined by inhomogeneous domain wall pinning. Different from the nanocomposite magnets with hard and soft magnetic phases, the reverse field, where the reversible susceptibility χ_{rev} peaks, is found to be 5.8 kOe, which is much lower than the field corresponding to the χ_{total} maximum. The study of magnetic viscosity indicates that the time dependence of magnetization is primarily determined by the reversal of $\text{PrCo}_5\text{C}_\delta$ phases, and a larger activation volume, $v=3.2 \times 10^{-18} \text{ cm}^3$, is deduced for the $\text{PrCo}_{4.5}\text{C}_{0.5}$ ribbons. © 2008 American Institute of Physics. [DOI: 10.1063/1.2939235]

I. INTRODUCTION

The magnetic hardening and remanence enhancement in nanocrystalline two-phase permanent magnets composed of hard and soft magnetic phases have been observed and studied extensively in the past decades,¹⁻³ and the so-called exchange coupling between magnetic hard and soft phases was supposed² to be the unique principle of all these phenomena. However, relatively limited investigations on the exchange coupling effects have been reported for the magnets composed of two different hard magnetic phases.⁴ In our previous work, $\text{PrCo}_{4.5}\text{C}_{0.5}$ ribbons with the uniform cellular $\text{PrCo}_5\text{C}_\delta/\text{Pr}_5\text{Co}_{19}\text{C}_\epsilon$ nanocomposite microstructure had been fabricated by the melt spinning technique.⁴ A coercivity of 6.1 kOe, a remanence ratio of 0.81, and a maximum magnetic energy product of 12.0 MGOe were obtained at room temperature. Although the high remanence ratio and the single magnetic phase behavior have been proven to arise from the exchange coupling between different hard phases, the exact mechanism of magnetic reversal in this kind of nanocomposites remains to be explored. In this paper, we performed a systematic study on the reversible and irreversible magnetization reversals and magnetic viscosity of the nanostructural $\text{PrCo}_{4.5}\text{C}_{0.5}$ ribbons, which will lead us to a deep understanding of the magnetic reversal process.⁵⁻¹⁰

II. EXPERIMENT

Alloy ingots with the nominal composition of $\text{PrCo}_{4.5}\text{C}_{0.5}$ were prepared by arc melting the raw materials Pr, Co, and C (with the purity better than 99.99%) in an argon atmosphere of high purity. An excess of 5 wt. % Pr was added to compensate for the loss during the melting. Nanostructural $\text{PrCo}_{4.5}\text{C}_{0.5}$ ribbons were obtained by directly melt spinning the resultant ingots $\text{Pr}_{1.1}\text{Co}_{4.5}\text{C}_{0.5}$ in argon atmosphere at an optimal wheel speed of 25 m/s. Magnetic

measurements of the $\text{PrCo}_{4.5}\text{C}_{0.5}$ ribbons, including the measurements of recoil curves, minor hysteresis loops, demagnetization curves, dc demagnetization remanence curves, and time-dependent magnetizations were performed using a vibrating sample magnetometer (LakeShore VSM 7410) with an applied magnetic field up to 24 kOe at room temperature.

III. RESULTS AND DISCUSSION

The recoil curves for the initial magnetization (M) process of the $\text{PrCo}_{4.5}\text{C}_{0.5}$ ribbons are shown in Fig. 1. It can be seen that the recoil curves remain steep with increasing applied field for $H/iH_c < 1$, where iH_c is the coercive force determined with the major demagnetization curve, and the reduced remanence $m_r(H)$ [defined as $J_r(H)/J_r^{\text{max}}$] is less than 0.5 at $H \approx iH_c$, where the remanence $J_r(H)$ is acquired after the application and subsequent removal of H , and J_r^{max} is the saturation remanence. The highly recoverable magnetization at low magnetic field with $H/iH_c < 1$ may primarily originate from the $\text{Pr}_5\text{Co}_{19}\text{C}_\epsilon$ phase. This will be discussed

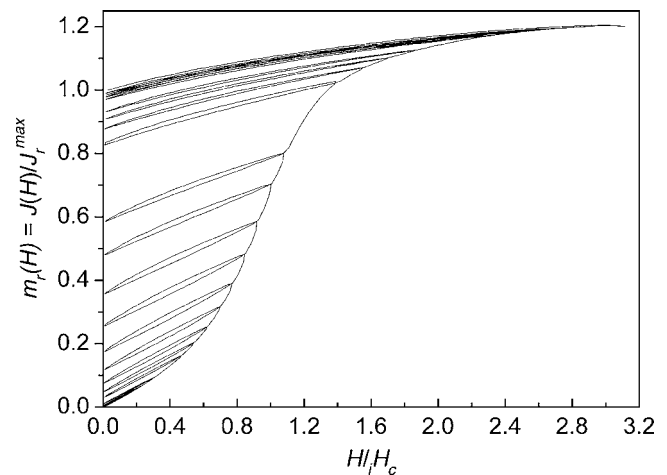


FIG. 1. Recoil curves in the initial magnetization process of the melt-spun $\text{PrCo}_{4.5}\text{C}_{0.5}$ ribbons at a wheel speed of 25 m/s.

^{a)}Author to whom correspondence should be addressed. Electronic mail: shenbg@g203.iphy.ac.cn.

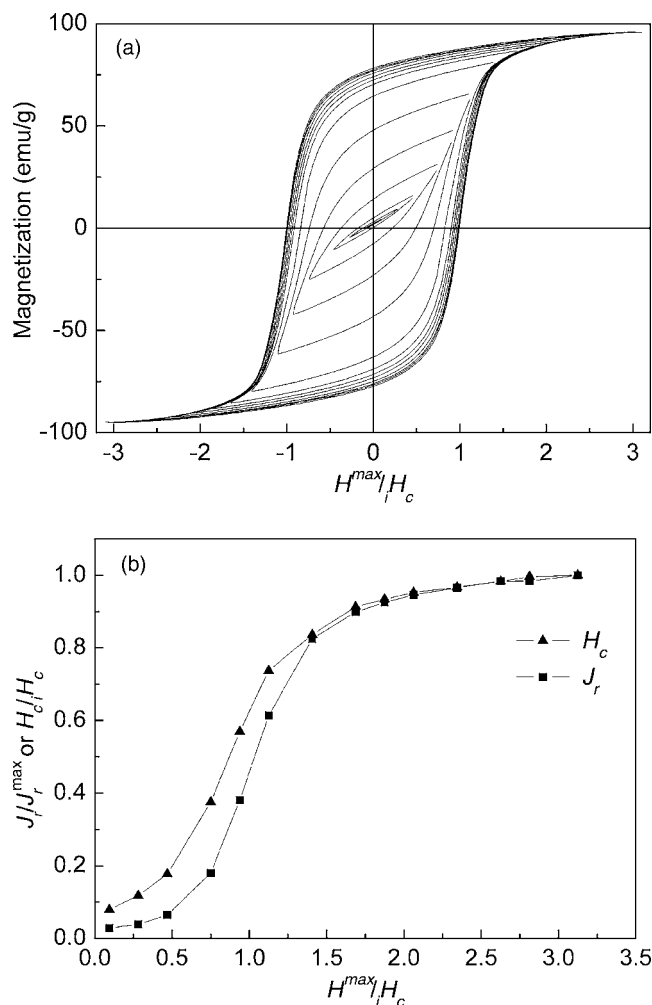


FIG. 2. Minor hysteresis loops (a) and the coercivity and remanence (b) as functions of the applied field H^{\max} of the melt-spun $\text{PrCo}_{4.5}\text{C}_{0.5}$ ribbons prepared at a wheel speed of 25 m/s.

further along with the reversible susceptibility χ_{rev} . Irreversibility appears and develops as magnetic field increases, and a $m_r(H)$ value larger than 0.8 is obtained for $H/iH_c > 1.3$. As can be also seen from Fig. 1, the value of magnetization in the initial M - H curve remains low until the applied field H exceeds a critical value. This implies that the coercivity of the $\text{PrCo}_{4.5}\text{C}_{0.5}$ ribbons is primarily governed by the domain wall pinning.^{11,12}

This feature can also be observed in the magnetization curves with minor hysteresis loops [Fig. 2(a)]. Asymmetrical minor hysteresis loops were observed at lower applied field of $H^{\max}/iH_c < 0.6$, where H^{\max} is the maximum applied magnetic field for certain minor loop, which may result from the pinning effect of domain wall movements during magnetization process.⁶ The typical features of domain wall pinning are that the coercivity and remanence are low and increase slowly when the applied field is low and grow rapidly after a critical field of $H^{\max}/iH_c > 1$ is reached [Fig. 2(b)]. Moreover, the low values of $J_r(H^{\max})/J_r^{\max} (< 0.8)$ even at $H^{\max}/iH_c \approx 1.2$ suggest the inhomogeneity of the domain wall pinning in $\text{PrCo}_{4.5}\text{C}_{0.5}$ ribbons, a phenomenon different from the ordinary model of domain wall pinning.¹³

A high degree of reversibility, as a criterion for the pres-

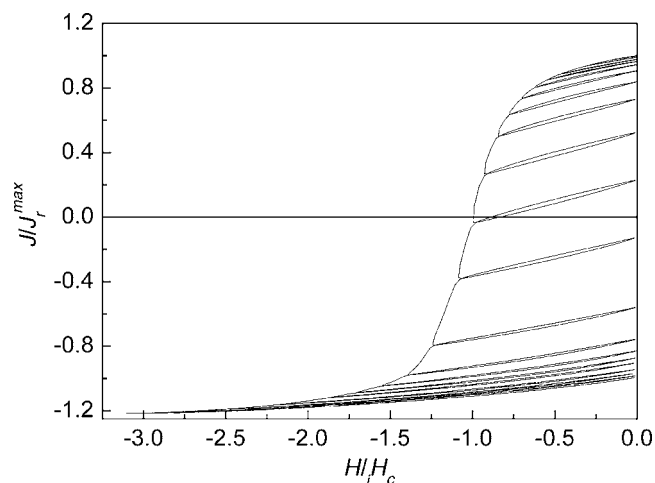


FIG. 3. Demagnetization curve and recoil loops of the melt-spun $\text{PrCo}_{4.5}\text{C}_{0.5}$ ribbons at a wheel speed of 25 m/s.

ence of exchange-spring mechanism,² was found in the demagnetization process with an applied field H lower than iH_c , as shown in Fig. 3. The quantities of $J_r(H)$ obtained from recoil curves during demagnetization process remain unchanged, nearly the same as the saturation remanence J_r^{\max} , even as the reverse field H approaches $0.6iH_c$. As demonstrated by the opening of recoil curves at the field around the coercivity, the irreversibility of magnetic reversal becomes obvious with further increasing magnetic field, which is a phenomenon similar to that observed for nanocomposite $\text{Pr}_2\text{Fe}_{14}\text{B}/\alpha\text{-Fe}$ magnets.¹⁴ As expected, the magnetizing characteristics in both the demagnetization and initial magnetization processes are consistent with each other in the vicinity of coercive force.

In order to deeply understand the process of magnetization reversal of $\text{PrCo}_{4.5}\text{C}_{0.5}$ ribbons, the $D(H)$ - H curves shown in Fig. 4(a) have been measured. $D(H)$ is the reduced irreversible portion of magnetization reversal, defined as $D(H) = -\Delta J_{\text{irr}}(H)/2J_r^{\max} = [J_r^{\max} - J_d(H)]/2J_r^{\max}$, where J_r^{\max} is the saturation remanence and $J_d(H)$ is the dc field demagnetization remanence acquired after saturation magnetized in one direction and subsequent application of a dc field H in the opposite direction. The critical field H_{n0} , i.e., the onset field required to stimulate the irreversible magnetization reversal, can be derived from the $dD(H)/dH$ - H curves.² As shown in the inset of Fig. 4(a), the value of H_{n0} for $\text{PrCo}_{4.5}\text{C}_{0.5}$ ribbons is 6.6 kOe, slightly larger than the coercivity (6.4 kOe). Similar result was also obtained for the nanocomposite $\text{Nd}_2\text{Fe}_{14}\text{B}/\text{Fe}_3\text{B}$ magnets,² while $H_{n0} < iH_c$ for the $\text{Pr}_2\text{Fe}_{14}\text{B}/\alpha\text{-Fe}$ exchange-coupled system.¹⁵ The differences among these nanocomposite magnets can be explained formally as due to the relative dimension of magnetic “soft” phase according to Kneller’s model.² The reduced reversible magnetization $-\Delta J_{\text{rev}}(H)/J_r^{\max}$ as a function of the reverse field H is given in Fig. 4(b) for comparison. A similar maximum is found in the $-\Delta J_{\text{rev}}(H)/J_r^{\max}$ - H curve for the nanocomposite $\text{Pr}_2\text{Fe}_{14}\text{B}/\alpha\text{-Fe}$ system.¹⁵

The total susceptibility χ_{total} and reversible susceptibility χ_{rev} , derived from the demagnetization curve and recoil loops, respectively,¹⁶ are shown in Fig. 5 as functions of the

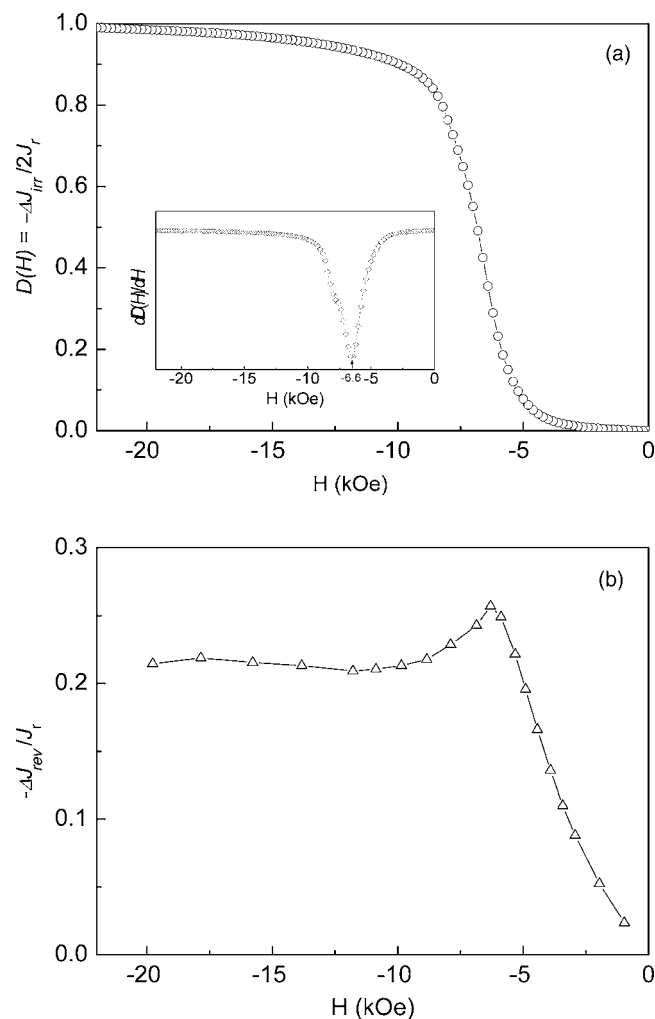


FIG. 4. The reduced quantity of irreversible portion $D(H)$ (a) and the reduced reversible magnetization $-\Delta J_{\text{rev}}(H)/J_r^{\text{max}}$ (b) as functions of the reverse field H for the $\text{PrCo}_{4.5}\text{C}_{0.5}$ ribbons.

reverse field H for the $\text{PrCo}_{4.5}\text{C}_{0.5}$ ribbons. A single maximum in $\chi_{\text{total}}-H$ curve can be found around the coercivity (6.4 kOe). The same feature has also been found for $\text{Nd}_2\text{Fe}_{14}\text{B}/\alpha\text{-Fe}$ nanocomposite system,¹⁷ but there are two maxima observed for the nanocomposite $\text{Sm}_2\text{Fe}_{14}\text{Ga}_3\text{C}_2/$

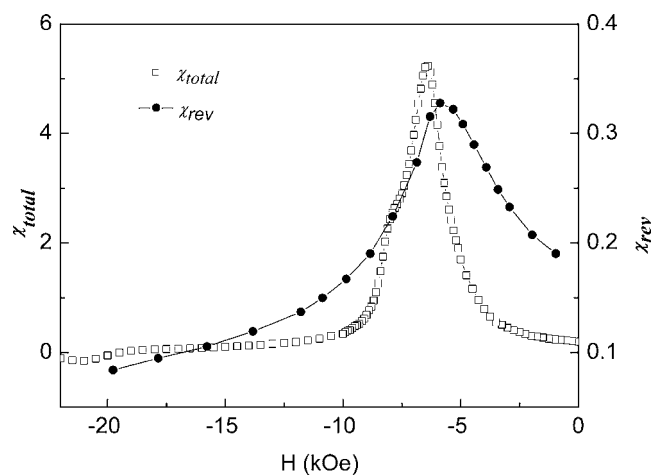


FIG. 5. The total susceptibility χ_{total} and reversible susceptibility χ_{rev} of the $\text{PrCo}_{4.5}\text{C}_{0.5}$ ribbons as functions of the reverse field H .

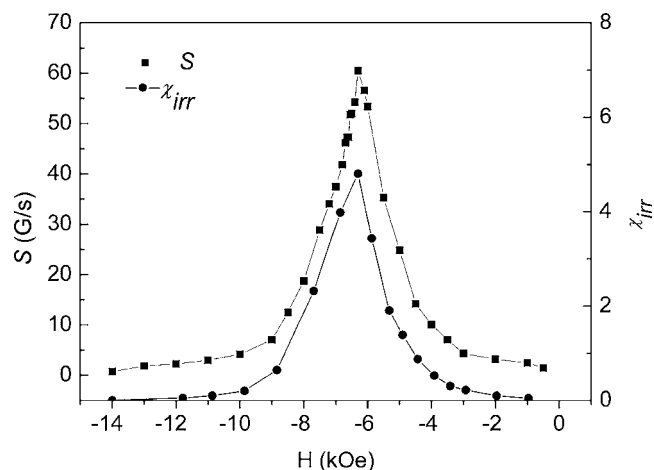


FIG. 6. Room-temperature magnetic viscosity coefficient S and irreversible susceptibility χ_{irr} as functions of the reverse field H .

$\alpha\text{-Fe}$ magnets.¹⁶ Furthermore, a single maximum is observed in the $\chi_{\text{rev}}-H$ curve in $\text{PrCo}_{4.5}\text{C}_{0.5}$ ribbons, which is a phenomenon similar to other nanocomposites.^{2,15-17} Considering the fact that the magnetocrystalline anisotropy field of $\text{Pr}_5\text{Co}_{19}\text{C}_e$ phase [about 38 kOe (Ref. 18)] is much lower than that of $\text{PrCo}_5\text{C}_\delta$ phase (about 170 kOe), it is reasonable to assume that $\text{Pr}_5\text{Co}_{19}\text{C}_e$ phase is comparatively magnetically “softer” than $\text{PrCo}_5\text{C}_\delta$ phase. The $\text{Pr}_5\text{Co}_{19}\text{C}_e$ phase may play the role of the magnetic soft phase, contributing to the reversible components of total magnetization during demagnetization process. These results are consistent with the mechanism proposed for magnetization reversal processes of the conventional two-phase nanocomposite magnets.²

Nevertheless, it should be noted that the field of 5.8 kOe, corresponding to the maximum of χ_{rev} , is much lower than the coercive force, where the χ_{total} curve exhibits a maximum. This seems to be the very difference between $\text{PrCo}_{4.5}\text{C}_{0.5}$ ribbons and nanocomposite $\text{Pr}_2\text{Fe}_{14}\text{B}/\alpha\text{-Fe}$ magnets, for the later both maxima of χ_{total} and χ_{rev} are located at almost the same field around coercivity.¹⁵ It could be due to the different magnetocrystalline anisotropy fields of $\text{Pr}_5\text{Co}_{19}\text{C}_e$ and $\alpha\text{-Fe}$ or the difference of microstructures. Much work is required for further clarity.

The magnetic viscosity arises from the thermal activation of magnetization reversal for overcoming energy barriers. The analysis of magnetic viscosity is expected to give deeper insight into the coercivity mechanism and the reversal mode of magnets.¹⁶ The measurements of magnetic viscosity were performed along the demagnetization curve by holding the applied field unchanged and recording the change of magnetization with time. The magnetic viscosity S can be obtained following the equation:⁹

$$J(t) = A + S \ln(t + t_0), \quad (1)$$

where $J(t)$ is the magnetization changing with time at a fixed applied field, t is the time since the applied field is held, and A and t_0 are constants. The viscosity coefficient $S = -dJ/d \ln t$ can be fitted to Eq. (1). The room-temperature magnetic viscosity coefficient S and irreversible susceptibility $\chi_{\text{irr}} = \chi_{\text{total}} - \chi_{\text{rev}}$ of $\text{PrCo}_{4.5}\text{C}_{0.5}$ ribbons are shown in Fig. 6 as functions of the reverse field H . Both the χ_{irr} and the S

curves exhibit maxima at approximately the same reverse field around coercivity. As mentioned above, the reversible magnetization reversal of $\text{PrCo}_{4.5}\text{C}_{0.5}$ ribbons primarily originates from the $\text{Pr}_5\text{Co}_{19}\text{C}_8$ phase, which induces a much lower reverse field as an indicative of the maximum of χ_{rev} versus H . Therefore, the time-dependent changes of magnetization should be primarily attributed to the magnetization reversal of PrCo_5C_8 phase rather than that of $\text{Pr}_5\text{Co}_{19}\text{C}_8$ phase.

The activation volume v , i.e., the magnetic switching volume, can provide information about the magnetic reversal behavior in magnets. According to Gaunt,¹⁹ $v = k_B T / H_f M_s$ for the typical domain wall pinning controlled magnets, where $H_f = S / \chi_{\text{irr}}$ is known as the fluctuation field and H_f is constant at a given temperature. The activation volume, $v = 3.2 \times 10^{-18} \text{ cm}^3$, has been estimated for the $\text{PrCo}_{4.5}\text{C}_{0.5}$ ribbons at room temperature. The equivalent diameter of sphere is assumed about 18 nm, which is roughly consistent with the cellular microstructure of the ribbons consisting of the PrCo_5C_8 phase with a grain size of 15 nm and $\text{Pr}_5\text{Co}_{19}\text{C}_8$ grain boundary phase in a width of 2 nm.⁴ The activation volume of the $\text{PrCo}_{4.5}\text{C}_{0.5}$ ribbons is larger than that [$1.4\text{--}2.8 \times 10^{-18} \text{ cm}^3$] of the single-phase PrCo_5 thin film magnets.²⁰ The existence of $\text{Pr}_5\text{Co}_{19}\text{C}_8$ phase in the $\text{PrCo}_{4.5}\text{C}_{0.5}$ ribbons may lower the pinning energy barrier in magnetic reversal process, resulting in a larger activation volume of the $\text{PrCo}_{4.5}\text{C}_{0.5}$ ribbons. Similar effect was also observed in the nanocomposite two-phase $\text{Pr}_2\text{Fe}_{14}\text{B}/\alpha\text{-Fe}$ magnets, whose activation volume v was much larger than that of the single-phase sintered $\text{Pr}_2\text{Fe}_{14}\text{B}$ magnet.¹⁵

IV. CONCLUSIONS

Magnetization reversal processes and magnetic viscosity of nanostructured $\text{PrCo}_{4.5}\text{C}_{0.5}$ ribbons composed of two hard magnetic phases $\text{PrCo}_5\text{C}_8/\text{Pr}_5\text{Co}_{19}\text{C}_8$ have been investigated. Large recoverable magnetization is observed in the $\text{PrCo}_{4.5}\text{C}_{0.5}$ ribbons, which is attributed to the presence of the $\text{Pr}_5\text{Co}_{19}\text{C}_8$ phase with relatively lower anisotropy field in comparison to the PrCo_5C_8 phase. A maximum of the reversible susceptibility χ_{rev} has been found at a reverse field of 5.8 kOe, much lower than the field indicative of the maximum of χ_{total} for the $\text{PrCo}_{4.5}\text{C}_{0.5}$ ribbons, which is different from the case of the conventional nanocomposite magnets

composed of hard and soft magnetic phases. The critical field H_{n0} for irreversible magnetization reversal is 6.6 kOe, slightly larger than the coercivity (6.4 kOe) for $\text{PrCo}_{4.5}\text{C}_{0.5}$ ribbons. The coercivity of the $\text{PrCo}_{4.5}\text{C}_{0.5}$ ribbons is primarily governed by inhomogeneous domain wall pinning. The time-dependent changes of magnetization have been determined dominantly by the magnetization reversal of $\text{Pr}_5\text{Co}_{19}\text{C}_8$ phases according to the measurements of magnetic viscosity of the ribbons. The activation volume of the $\text{PrCo}_{4.5}\text{C}_{0.5}$ ribbons is larger than those of single-phase PrCo_5 thin film magnets, which probably results from the presence of $\text{Pr}_5\text{Co}_{19}\text{C}_8$ phase.

ACKNOWLEDGMENTS

This work is supported by the National Natural Science Foundation and the National Basic Research Program of China.

- ¹R. Coehoorn, D. B. Mooij, and C. De Waard, *J. Magn. Magn. Mater.* **80**, 101 (1989).
- ²E. F. Kneller and R. Hwaig, *IEEE Trans. Magn.* **27**, 3588 (1991).
- ³R. Skomski and J. M. D. Coey, *Phys. Rev. B* **48**, 15812 (1993).
- ⁴B. Yang, B. G. Shen, T. Y. Zhao, and J. R. Sun, *J. Phys. D: Appl. Phys.* **41**, 015003 (2008).
- ⁵I. Panagiotopoulos, L. Withanawasam, and G. C. Hadjipanayis, *J. Magn. Magn. Mater.* **152**, 353 (1996).
- ⁶H. W. Zhang, T. Y. Zhao, C. B. Rong, S. Y. Zhang, B. S. Han, and B. G. Shen, *J. Magn. Magn. Mater.* **267**, 224 (2003).
- ⁷J. E. Shield, J. Zhou, S. Aich, V. K. Ravindran, R. Skomski, and D. J. Sellmyer, *J. Appl. Phys.* **99**, 08B508 (2006).
- ⁸D. Givord, P. Tenaud, T. Viadieu, and G. C. Hadjipanayis, *J. Appl. Phys.* **61**, 3454 (1987).
- ⁹E. W. Singleton and G. C. Hadjipanayis, *J. Appl. Phys.* **67**, 4759 (1990).
- ¹⁰D. C. Crew, P. G. McCormick, and R. Street, *IEEE Trans. Magn.* **32**, 4356 (1996).
- ¹¹F. E. Pinkerton and D. J. Van Wingerden, *J. Appl. Phys.* **60**, 3685 (1986).
- ¹²J. F. Liu, H. L. Luo, and J. Wan, *J. Pediatr. (St. Louis)* **25**, 1238 (1992).
- ¹³K. H. J. Buschow, *Rep. Prog. Phys.* **54**, 1123 (1991).
- ¹⁴D. Goll, M. Seeger, and H. Kronmüller, *J. Magn. Magn. Mater.* **185**, 49 (1998).
- ¹⁵H. W. Zhang, W. Y. Zhang, A. R. Yan, and B. G. Shen, *Acta Phys. Sin.* **48**, S212 (1999).
- ¹⁶E. H. Feutrill, P. G. McCormick, and R. Street, *J. Phys. D: Appl. Phys.* **29**, 2320 (1996).
- ¹⁷J. Ding, Y. Li, and K. Y. Li, *J. Phys.: Condens. Matter* **10**, 9081 (1998).
- ¹⁸A. E. Ray and K. J. Strnat, *IEEE Trans. Magn.* **MAG-11**, 1429 (1975).
- ¹⁹P. Gaunt, *J. Appl. Phys.* **59**, 4129 (1986).
- ²⁰S. S. Malhotra, Z. S. Shan, D. C. Stafford, S. H. Liou, and D. J. Sellmyer, *IEEE Trans. Magn.* **32**, 4019 (1996).